ACS Partner Journal

ACCOUNTS of materials research

pubs.acs.org/amrcda Article

Microstructure Dictating Performance: Assembly of Graphene-Based Macroscopic Structures

Mingxin Li and Jie Lian*

Cite This: *Acc. Mater. Res.* 2021, 2, 7−20 Read Online

ACCESS | Metrics & More | Article Recommendations

CONSPECTUS: A wide range of groundbreaking advancements in electronics, photonics, nanocomposites, etc., have been achieved in the past decades due to the favorable attributes of single-layer graphene, including its record-breaking thermal conductivity, charge carrier mobility, fracture strength, and Young's modulus. However, the realization of the potentials of macroscale graphene assemblies has remained challenging. The difficulties mainly lie within manipulating graphene sheets into an orderly intermolecular orientation and controlling the macroscopic ordering of the graphitic domains. Controlling the formation of graphene macroscopic structures and eliminating defects on both the nano- and microscales meanwhile optimizing performance is no easy feat. To address these microstructural issues in macroscopic graphene assemblies, multiple chemical, thermal, and mechanical approaches have been developed with a goal of overall performance enhancement. Therefore, in this Account we provide a brief review of our contributions in the microstructure engineering of macroscale graphene assemblies with the focus on graphene fibers (GFs), graphene papers (GPs), and other graphene-based assemblies with graphene oxide (GO) colloids as precursors.

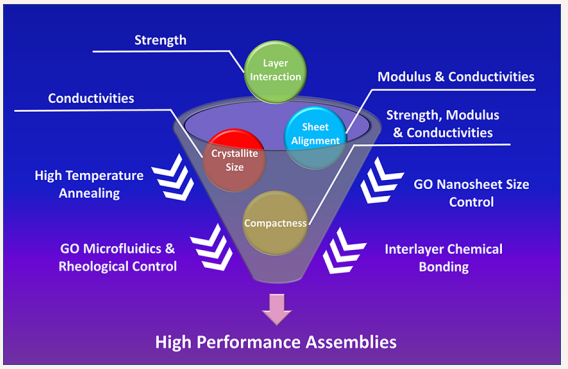

Building upon the developments in wet chemistry on assembling individual GO sheets into macroscopic structures, we successfully intercalated large GO sheets with small GO sheets, which increased compactness for wet-spun GFs without disturbing the sheet orientation and alignment of the large GO sheets. Increasing GO compactness during wet assembly allows for the increase of thermal and electrical conductivities as well as the mechanical strength of GFs at a single stroke. A high degree of alignment of graphene sheets with abundant sp^2 carbon atoms is also necessary for achieving high thermal and electrical conductivities in graphene assemblies. Fine control of GO sheet alignment and orientation during the wet-spinning assembly is demonstrated through the shape and size confinement of fluidic flow channels. Utilizing this shear-stress-induced self-alignment strategy, the core−shell nonuniformity problem of GFs is addressed. Also, a correlation between the rheological properties and flow patterns of GO during wet-spinning and the microstructure of the GF assemblies is established.

In addition to the orientation of graphene sheets, the crystallite size and macroscopic ordering within graphene assemblies also play important roles in determining their performances. Larger and highly oriented graphitic crystalline domains allow for higher thermal and electrical conductivities. By manipulating crystallite domain size and arrangement through high temperature graphitization, the electrical and thermal conductivities and Young's modulus of GFs can be significantly enhanced. Fine temperature control can also help retain residual covalent cross-links between neighboring graphene sheets, meeting the need for balancing tensile strength, and thermal and electrical conductivities.

The enhancement of GF mechanical, thermal, and electrical properties through optimizing the compactness and alignment of graphene sheets and the orientation of graphene crystallite domains have significantly improved the engineering capability of GFs. Such an improvement has been largely beneficial to flexible electronics research and has shown great potential in multifunctional composite materials. Similar strategies have also been emulated on related graphene-based materials such as graphene papers (GPs) and graphene fiber meshes (GFMs), yielding unique and favorable properties and performances.

1. INTRODUCTION

The bottom-up assembly of nanoscale materials into microscale structures and macroscale devices has long been an appealing goal in the field of nanotechnology. Of the wide range of nanomaterials developed in the past four decades, graphene has become one of the most promising and favorable

Received: October 10, 2020
Revised: December 7, 2020
Published: December 15, 2020

https://dx.doi.org/10.1021/accountsmr.0c00053
Acc. Mater. Res. 2021, 2, 7−20

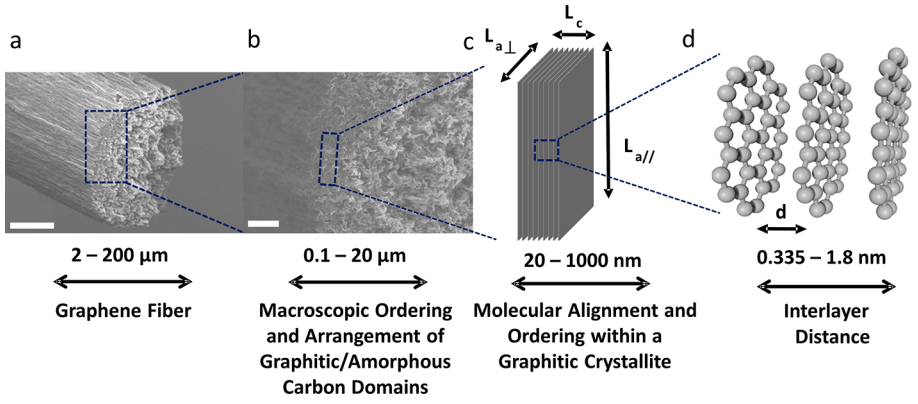

Figure 1. Molecular orientation (graphene sheet alignment) and macroscopic ordering of crystalline graphitic domains within the macroscopic graphene structures. Top-down from (a) to (d): (a) macroscopic GFs (reproduced with permission from ref 6; copyright 2019 Springer Nature); (b) macroscopic ordering and arrangement of graphitic amorphous carbon domains (reproduced with permission from ref 6; copyright 2019 Springer Nature); (c) molecular alignment and ordering of graphene sheets within a graphitic crystallite; (d) interlayer distance between individual graphene layers. Scale bars, 5μm (a) and 1μm (b).

materials due to its extraordinary physical features and rich chemistry. Among its different assembly approaches, significant breakthroughs have been achieved using the fluid assembly of GO sheets into macroscopic materials, including fibers (1D), papers (2D), and aerogels (3D).[1−3]

Before the advent of macroscopic graphene materials, low density, high strength, and high stiffness carbon fibers (CFs) were indisputably the most prominent members in the family of macroscale carbon materials. In 2011, with the development of a facile wet-spinning approach for assembling GO fibers (GOFs) from GO dispersions and various methods for subsequently reducing GOFs, GFs emerged as an alternative carbonaceous macroscale fiber material to conventional mesophase pitch-based (MPP-based) and polyacrylonitrile-based (PAN-based) CFs in the CF family.[1] Compared to conventional CFs, the rich chemistry and intriguing fluid properties of the fluid GO precursors have allowed for the versatile assembly of GFs with tunable mechanical properties.[4] Meanwhile, graphene's outstanding electron and phonon transport properties have also made a mark on the superior performance of GFs.[5] In recent years, significant research efforts on the assembly process have allowed the assembled macroscopic graphene structures to mostly maintain excellent physical, thermal, and electrical properties of individual graphene sheets. High-performance GFs are now outperforming the best conventional CFs in both thermal and electrical conductivities.[5,6] In terms of mechanical properties, some GFs can come on par with some commercially available CFs.[7] In contrast, others have been engineered to be highly flexible,[8] presenting a high degree of tunability.

Despite these recent advancements, the overall goal of fabricating GFs to realize outstanding mechanical, thermal, and electrical performances simultaneously remains challenging. On the microscale, the requirements for mechanical strengthening and thermal and electrical conductivity enhancement pose an apparent conflict. The abundance of highly aligned sp^2 graphene sheets is beneficial for high thermal and electrical transports in GFs. Yet, the mechanical interaction between these sp^2 graphene sheets is limited due to their relatively weak van der Waals interactions.[5,9] Cross-links can enhance the mechanical interaction between graphene sheets. However, the sp^3 cross-linking bonds also behave as effective phonon and electron scattering centers, thus decreasing thermal and electrical conductivities.[10,11] The skin effect that typically occurs during the wet-spinning assembly of GOFs translates to a core−shell structure in GFs after chemical or thermal reduction.[6] The random graphene sheet alignment within the fiber core leads to a turbostratic arrangement of graphitic domains in the transverse direction.[11] These domains with low crystallinity, small crystallite size, and an abundance of pinhole defects and structural flaws significantly impede the phonon and electron transport in GFs.[6]

GPs have also become transformative macroscale 2D materials due to their high aspect ratio, ease of assembly, and the potential to compete with bucky papers and carbon nanotube papers. For functional applications, mechanical and electrical property enhancement through microstructural improvements, including compactness enhancement and interfacial cross-linking, has been a priority of GP research. GP compactness has been successfully improved by various methods, e.g., by introducing soft porous GO sheets as a binder to improve interlayer packing and load transfer,[12] mixing rGO nanoflakes with GO sheets to assist GO densification during graphitization, and introducing other small sized 2D nanosheets between GO sheets to densify graphene oxide papers (GOPs) prior to their reduction into GPs.[13−17] All these strategies resulted in densified microstructures within GPs and improved their toughness and mechanical strength. To simultaneously improve the mechanical and electrical performances of GPs, a number of interfacial cross-links, including covalent bonding, $\pi-\pi$ bonding, and ionic bonding, have been used in combination with each other.[18−21] However, despite the improvements that have been brought by these efforts, there is much space for further enhancing the performance of GPs, particularly with respect to their thermal conductivity.

In this Account, we discuss the strategy of multiscale graphene-based assembly optimization, particularly molecular orientation and macroscopic ordering (as shown in Figure 1). Different methods that simultaneously enhance mechanical, electrical, and thermal properties on the atomic-, nano-, and microscales are highlighted. Key aspects of materials control and processing mainly include the controls and manipulations of (1) GO sheet size, (2) alignment of the GO sheets during fluidic flow-assisted assembly, and (3) high temperature annealing of GFs. Each of these methods focuses on improving

https://dx.doi.org/10.1021/accountsmr.0c00053
Acc. Mater. Res. 2021, 2, 7−20

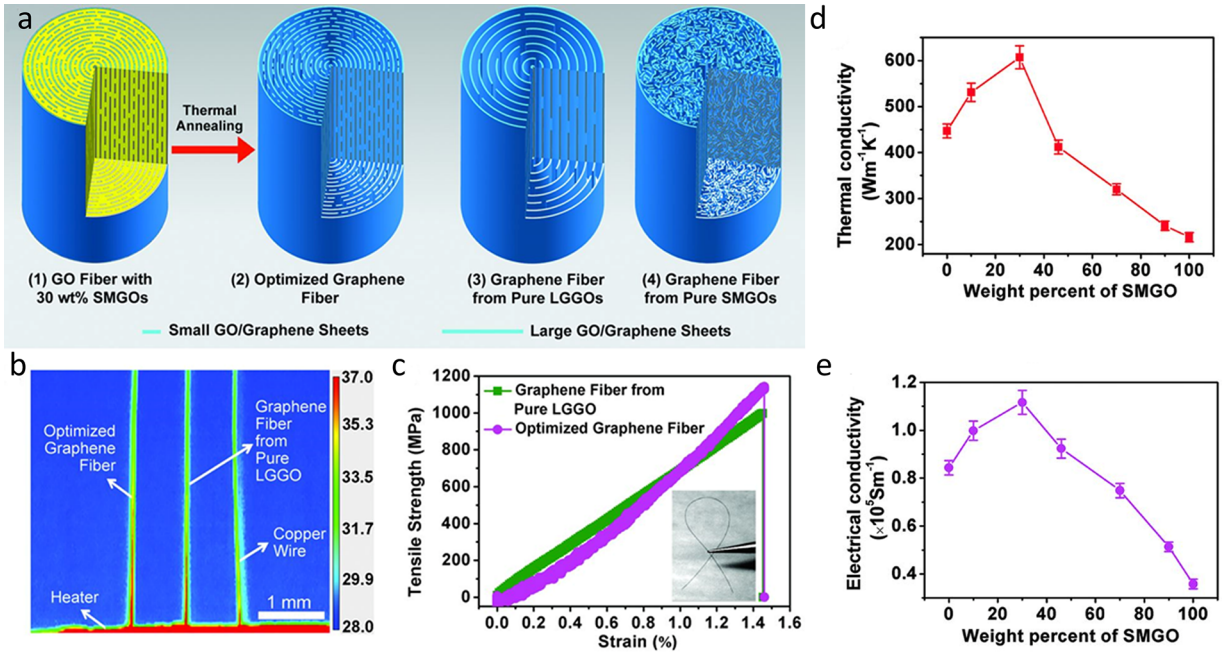

Figure 2. Highly thermally and electrically conductive and mechanically strong GFs (reproduced with permission from ref 5; copyright 2015 American Association for the Advancement of Science): (a) schematics of GOFs and GFs with an "intercalated" structure of large and small-sized graphene sheets; (b) and (c) greatly enhanced thermal transport and mechanical strength of the optimized GFs; (d) and (e) optimization of thermal and electrical conductivities with various degrees of SMGO intercalation.

one or more of the four major materialistic aspects that determine the performance of GFs, including layer interaction between graphene sheets, GO/graphene sheet alignment, GO/graphene sheet compactness, and graphitic domain size, crystallinity and macroscopic ordering. These four materialistic aspects govern the quality of performance in many other graphene-based assemblies in general. In our work, we also touch upon the development of GPs and GFMs with unique performances based upon the same materialistic improvement principles. The scientific significance and application potentials of these efforts of multiscale structural optimization of GFs and other graphene-based assemblies are also highlighted.

2. GRAPHENE OXIDE SHEET SIZE CONTROL

Liquid-phase chemical exfoliation of graphite involves the chemical introduction of functional groups onto its graphene layers. These functional groups weaken the van der Waals force between functionalized graphene layers, thus forming dispersions, most commonly in the form of GO.[4] Liquid-phase chemical exfoliation has proven to be an excellent method of producing GO precursors for graphene-based assemblies thanks to its scalability, versatility, rich chemistry, and the easy processability of GO in its liquid phase.[4] As the lateral size of single-layer GO sheets directly corresponds to their molecular weight, through isopycnic differential centrifugation, GO sheets with a lateral size approaching 100 μm can be selected.[22] Smaller GO sheets, down to the submicrometer scale, can either be obtained by tuning the centrifugation process and selecting the upper layers of the centrifuged GO colloid or through sonicating dispersions of larger GO sheets.[5]

2.1. GFs with GO Precursors of Large Sheet Sizes

Prior to the development of the GF wet-spinning assembly method, studies on mechanical properties of carbon nanotube fibers (CNTFs) have revealed that lateral interactions between adjacent carbon nanotubes (CNTs) increase as their aspect ratios increase. This in turn leads to the increase in the CNTFs' overall tensile strength.[23] The alignment of CNTs within CNTFs was also identified as a factor influencing their mechanical performance. Better alignment of these CNT building blocks contributed to their higher tensile strength and Young's moduli.[24]

As a similar assembly of high aspect ratio nanocarbons, early GFs had electrical conductivities comparable to most PAN-based CFs and orders of magnitude higher than that of graphene polymer composite fibers.[1] However, their tensile strength of less than 200 MPa and Young's moduli of less than 10 GPa were considerably lower than these of the high performance CNTF and CF counterparts.[1,25,26]

Inspired by the mechanical property improvement of CNTFs through increasing the aspect ratio of individual CNTs, Xu et al. successfully increased the tensile strength of GOFs to 364.4 MPa by using giant graphene oxide (GGO) sheets as the wet-spinning precursor. The average lateral size of the GGO sheets was 18.5 μm, with the largest sheets reaching 42 μm. After chemical reduction by hydroiodic acid, the oxygen functional groups on the GGO sheets were partially removed, decreasing interlayer spacing, leading to increased interlayer van der Waals interaction while preserving the hydrogen bonding between residual functional groups. Consequently, the tensile strength of the resulting GFs was further increased to 501.5 MPa, and the Young's modulus reached 11.2 GPa.[22] In graphene assemblies, the electrical resistance between adjacent graphene sheets is larger than that within an individual graphene sheet.[27] This leads to the 40% increase of electrical conductivity compared to GFs assembled from small graphene sheets, since using GGO building blocks reduces the sites of high interlayer resistance in a GF.[22]

https://dx.doi.org/10.1021/accountsmr.0c00053
Acc. Mater. Res. 2021, 2, 7−20

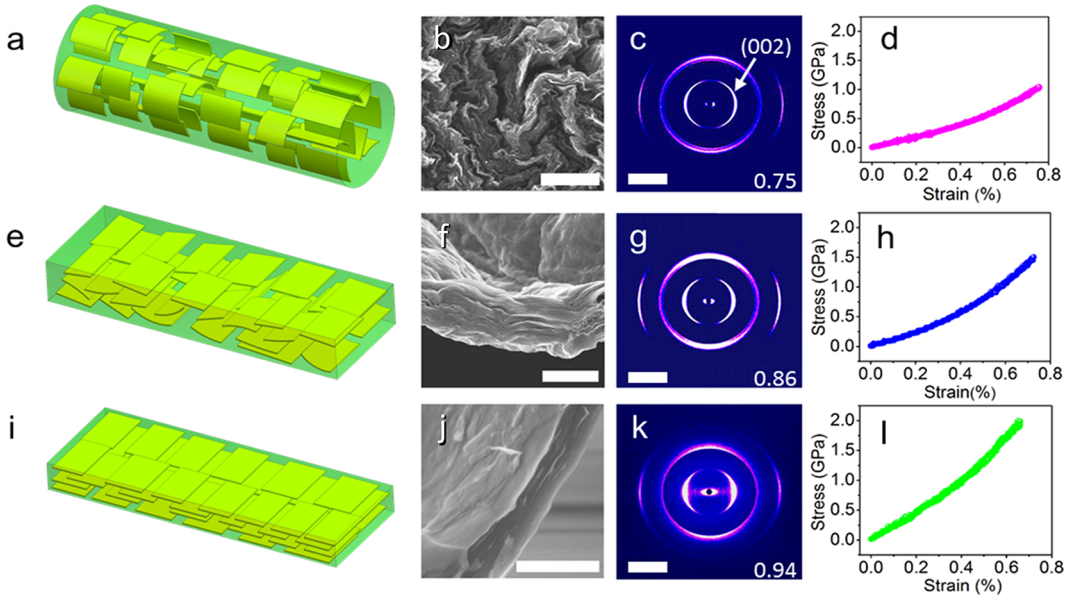

Figure 3. Shape and size confinements of graphene macroscopic structures by microfluidics-assisted assembly (reproduced with permission from ref 6; copyright 2019 Springer Nature): (a, e, i) GO sheet alignments during fluid flows inside microchannels with different geometries and aspect ratios and (b, f, j) corresponding microstructures, revealed by SEM images; (c, g, k) graphene sheet alignment by WAXS and (d, h, l) the mechanical properties of the resulting graphene-based macroscopic structures. Scale bars, 1μm (b), 1μm (f), 0.5 μm (j), and 20 nm^{-1} (c), (g) and (k), respectively.

2.2. GF Performance Optimization by Blending GO Sheets of Large and Small Sizes

The employment of GGO sheets as the building blocks for GFs significantly increases the interaction between individual sheets, contributing to the improvement in mechanical and electrical properties. However, careful examination of GGO GFs under small-angle X-ray scattering (SAXS) reveals strong equatorial streak patterns. These patterns indicate slit-shaped microvoids with a high aspect ratio well-aligned to the fiber axis. During the subsequent chemical and thermal reduction process, the removal of oxygen-containing functional groups in the form of gaseous H_2O, CO, and CO_2 causes the formation of these microvoids, further causing GGO GFs to have lower than optimal compactness and introducing electron and phonon scattering points. As a result, further improvement of the mechanical, thermal, and electrical properties of GGO GFs is greatly hindered.[5]

Understanding the importance of eliminating microvoids within GFs and increasing fiber compactness, we proposed mixing small-sized GO (SGO) (average lateral size 0.8 μm) with GGO (average lateral size ~23 μm) before wet-spinning to form new GFs with SGO sheets intercalated between GGO sheets (Figure 2). The intercalated SGO would occupy the locations within the GFs where microvoids would have formed otherwise, leading to an increase in compactness of GF microstructures.[5] This is corroborated by the deformation of the SAXS equatorial streak from patterns showing strong anisotropy to isotropic ellipse patterns, suggesting the transformation to a random distribution of the remnant slit-shaped microvoids.[5] The addition of SGO with low aspect ratios increases the overall misalignment of graphene sheets but poses no impediment to the physical properties of GFs. Thus, to achieve optimal performance, the addition of 30 wt % SGO was experimentally determined and recommended. Upon thermal annealing at 2850 °C, whose effect will be touched upon in section 5, the thermal and electrical conductivities and Young's modulus achieved 1290 W m^{-1} K^{-1}, 2.21 × 10^5 S m^{-1}, and 135 GPa, respectively. These values show 29%, 23%, and 35% improvement compared to that of pure GGO GFs thermally annealed at the same conditions. The maximum tensile strength of 1080 MPa was achieved upon thermal annealing at 1800 °C, 14% greater than the highest tensile strength achieved by GGO GFs thermally annealed at 1600 °C.[5,22]

3. MICROFLUIDIC MANIPULATION OF GRAPHENE OXIDE SHEETS

Besides improving fiber compactness, another important materialistic factor for enhancing GF performance is improving graphene sheet alignment. The balance between alignment and compactness is taken into consideration when optimizing the weight percentage of SGO in the wet-spinning precursor mixture.[5] Yet in pure GGO GFs and optimized GFs alike, it can be observed that within the core of these GFs, there is a lower degree of graphene sheet alignment compared to the outer layers. Along with high porosity and rough cross-sectional morphology of the GF core, this difference in graphene sheet alignment is indicative of a core−sheath structure commonly seen in GFs.[6,7]

3.1. GO Sheet Alignment Control through Microchannel Size and Shape Confinement

During the wet-spinning process, GO sheets are prompted by a shear force to align along the flow direction. Within a tubular spinneret, the shear force that induces alignment is stronger near the spinneret inner wall and weaker at the center of the flow. This difference in alignment along the transverse direction of the flow is preserved through subsequent GF fabrication processes of coagulation and reduction, translating into a core−sheath structure in GFs. Heavily wrinkled graphene sheets randomly aligned within the fiber core,

https://dx.doi.org/10.1021/accountsmr.0c00053
Acc. Mater. Res. 2021, 2, 7−20

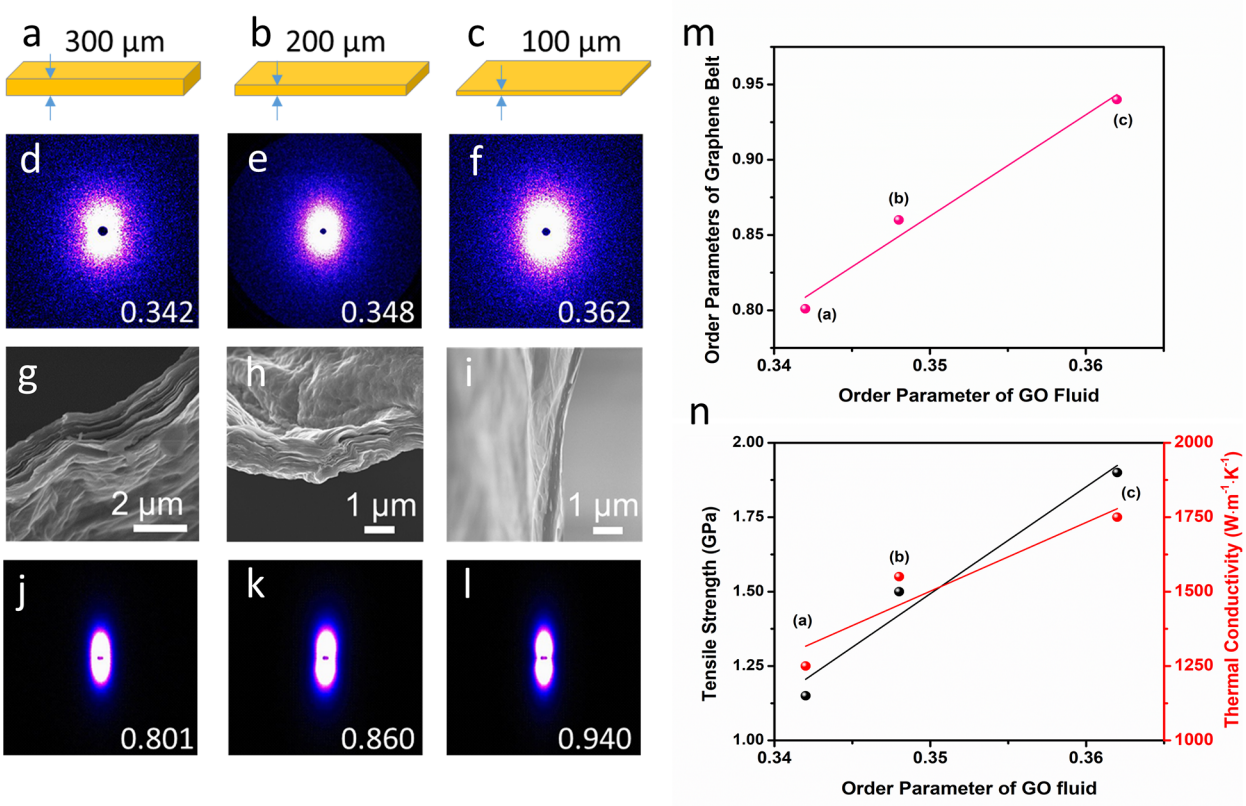

Figure 4. Process−structure−property correlations of the graphene belt structure by microfluidics-assisted assembly (reproduced with permission from ref 6; copyright 2019 Springer Nature): (a)−(c) schematic drawings of microchannels with different heights; (d)−(f) in situ SAXS patterns acquired from GO fluids inside microchannels in (a)−(c); (g)−(i) microstructure of the annealed graphene belts wet-spun from microchannels in (a)−(c); and (j)−(l) corresponding SAXS patterns; (m) a linear correlation of the orientation parameter of GO fluid flow and the order parameter of the final resultant graphene belts determined from SAXS; (n) linear correlations of the orientation parameter of GO fluid flow and the tensile strength and thermal conductivity of the final resultant graphene belts.

forming turbostratic crystallite domains instead of fully graphitic ones. Microvoids on the fiber cross-section are overwhelmingly found in the fiber core.[6,7]

Tubular spinnerets have cross sections with a low circumference to area ratio of 4:*D*, where *D* is the inner diameter of the spinneret, usually at around 100 μm. By employing a smaller tubular spinneret, Xu et al. were able to fabricate ultrastrong GFs with a cross-sectional diameter of less than 2 μm using a low concentration GO dispersion.[7] The core to sheath ratio within the cross sections of these thin GFs is significantly smaller than that of GFs with larger diameters.

To further reduce core to sheath ratio, our group used flat microchannels that are geometrically compatible with GO sheets as spinnerets (Figure 3e,i).[6] Graphene belts were wet-spun from these flat microchannel spinnerets. Examination of the microstructure of anisotropic graphene belts reveals much-improved sheet alignment (Figure 3f,j) and a complete absence of turbostatically arranged crystallite cores as seen in tubular fibers with a core−sheath structure (Figure 3b). Enhanced sheet alignment of the graphene belts is further confirmed by the narrow dispersion of the (002) plane on their wide-angle X-ray scattering (WAXS) patterns (Figure 3g,k).[10]

To understand how different processing parameters including GO concentration, flow rate, and the dimensions and shape of the microfluidic channels affect the alignment of GO sheets in fluids and graphene sheets in final resultant graphene belts, in situ SAXS was performed to determine the GO sheet orientation inside the GO flows within the microchannels. It was found that as the heights of the microchannels decreased (Figure 4a−c), the SAXS patterns for the GO flows became more anisotropic (Figure 4d−f).[6] SAXS patterns with a higher degree of anisotropy indicate a higher degree of GO sheet orientation within the microchannel. The GO sheet orientation can be quantified by converting the orientation distribution into a Hermans order parameter.[6] At the same flow velocity and volumetric flow rates, SAXS patterns of GO flows from flat microchannels with lower aspect ratios are more anisotropic than that of GO flows from tubular microchannels, corresponding to a higher Hermans order parameter and a higher degree of GO sheet orientation due to the enhanced shear stress along the channel wall.[6] Increasing flow rates also increases the shear stress applied to GO sheets in the microchannel, improving the sheet orientation initially until saturated at higher flow rates.[6]

The orientation order of GO sheets in a microchannel flow can be preserved and is directly transferred to a higher degree of alignment of the graphene sheets in the final resultant graphene belts. High Hermans order parameters of the obtained graphene belts indicate a strong impact that GO sheet alignment control during the fluidic-assisted assembly process has on microstructure optimization (Figure 4g−m) and performance enhancement (Figure 4n).[6] A positive linear correlation can be found between the Hermans order parameter of the GO flows in flat microchannels, the order parameter of the graphene sheets, and the resulting tensile strength and thermal conductivity of the graphene belts. The

https://dx.doi.org/10.1021/accountsmr.0c00053
Acc. Mater. Res. 2021, 2, 7−20

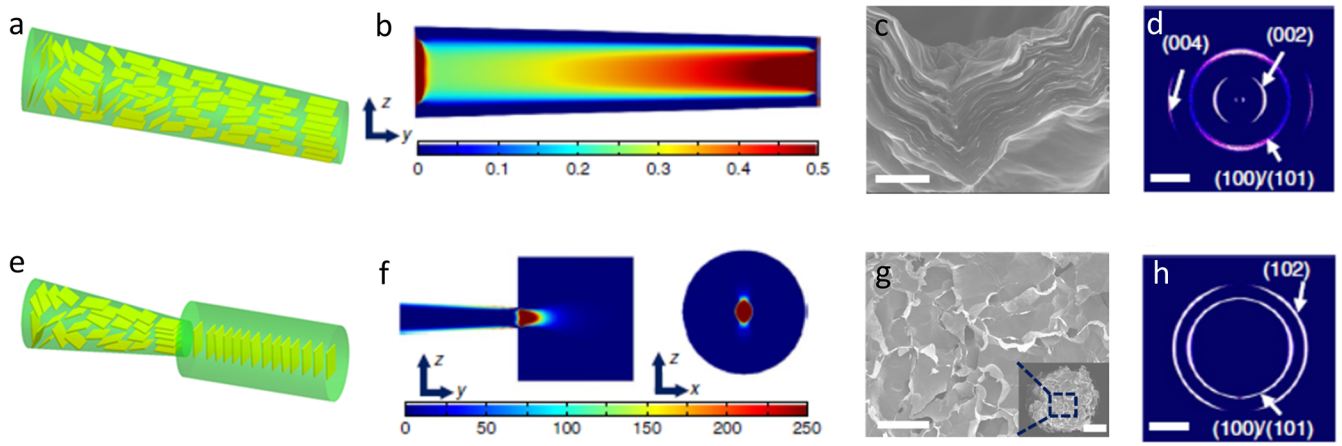

Figure 5. Control of flow patterns from contraction and step-expansion flows to control molecular orientation and macroscopic ordering of the GO and graphene sheets in the fluid flow and annealed GFs wet-spun from the corresponding fluidic flows (reproduced with permission from ref 6; copyright 2019 Springer Nature): (a, e) schematics of GO orientation during fluid flow from contraction and step-expansion patterns; (b, f) computational fluid dynamic simulations of the calculated elongation rates of GO; (c, g) microstructure and graphene sheet orientation; (d, h) corresponding WAXS patterns showing structural orientation and arrangement of the graphene sheets in thermally annealed GFs. Scale bars, 0.5μm (c), 200μm (g), 500μ (inset of g), and 20nm^{-1} (d) and (h), respectively.

optimized tensile strength and Young's modulus reach 1.9 GPa (Figures 3l and 4n) and 309 GPa, respectively, for the graphene belts with well-aligned graphene sheets and an order parameter of 0.94.[6]

The underlying mechanisms of size and shape confinement in tubular (Figure 3a) and flat microchannels (Figure 3e,i) are further analyzed by computational fluid dynamics simulations. According to simulation results, circularly distributed shear stress between geometrically mismatched 2D GO sheets and tubular channels tend to roll GO sheets to match the shear stress profile. Counteracted by the movement of GO sheets in the nematic phase, this effect leads to heavy wrinkling and distortion of the GO sheets, which results in GO sheets misaligning from the channel axis. When flowing within a flat channel, the degree of deformation and rotation of GO sheets depends on the difference in the lateral dimensions of the GO sheet and microchannels. When the lateral size of the GO sheets is much smaller than the channel size, the dimensional discrepancy allows for the rotation of GO sheets within the microchannels. When the lateral size of GO sheets approaches that of the microchannel, deformation and rotation of GO sheets are geometrically limited. The strong size and shape confinement leads to high degrees of orientation of GO sheets in fluidic flow. The overall shear-thinning phenomenon of GO within flat microchannels also reduces interactions between GO sheets, limiting the disturbance on alignment from each other during the microfluidic-assisted assembly process.[6]

3.2. Assembling Graphene Structure by Contraction and Step-Expansion Flows

In 2012, contraction and step-expansion flows were successfully used by Kiriya et al.[28] to manipulate the orientation of microfibers within a sol−gel fiber assembly. It was found that contraction flows facilitated the alignment of microfibers along the flow direction, while step-expansion flows reoriented microfibers perpendicular to the flow direction. Cylindrical polymeric micelles also reoriented perpendicularly to the flow after passing through a step-expansion flow, as observed by Trebbin et al. in 2013.[29] Further confirmation was given that this reorientation was stable.[30] If not modulated, micelles would propagate downstream in the perpendicular orientation.

Both the microfibers studied by Kiriya et al.[28] and the polymeric micelles studied by Trebbin et al. were liquid crystal-forming nanoparticles with high aspect ratios.[29,30] Prompted by the similarities they have with GO sheets, our group looked into the possibility of further tailoring the graphene sheet orientation in GFs by introducing contraction and step-expansion flows into the wet-spinning process.[6] Specifically, contraction flows were created by directing GO through a microchannel with a contracted cross-section along the flow direction (Figure 5a), and step-expansion flows were created by pumping GO from a contracted channel into a suddenly expanded channel (Figure 5e).

For the contraction flow, the gradual reduction of the channel cross-sectional area increases the elongation rate and flow rate in the flow direction. This results in increased shear stress and decreased viscosity of the GO flow (Figure 5b), which are favorable for improving GO sheet alignment. Analysis of SAXS patterns also shows that the less anisotropic pattern of the GO at the inlet drastically narrows into a strip as it approaches the center of the channel, indicating a significant improvement in GO sheet alignment. After this alignment is saturated at the midpoint through the channel, the narrow SAXS pattern remains unchanged until the outlet of the channel. WAXS patterns of graphene tubes wet-spun from a contraction flow show narrowly dispersed arcs of the (002) plane (Figure 5d), further confirming the effect of contraction flow on ensuring high sheet orientation in the resulting macroscale graphene assembly.[6,10]

For the step-expansion flow, the sudden inflation of the microchannel induces high extensional rates at the inlet of the expanded section (Figure 5f), leading to the rearrangement of GO sheets perpendicular to the flow direction. This is supported by the 90° rotation of the major axis of the SAXS pattern of the GO solution before and after the inlet of the expanded section. SEM observation shows the vertical alignment of the graphene sheet perpendicular to the axial direction of the final graphene rods (Figure 5g). WAXS patterns of graphene rods wet-spun from step-expansion flow channels show clear equatorial arcs of the (100)/(101) and (102) planes, while (002) and (004) scattering planes in GFs

https://dx.doi.org/10.1021/accountsmr.0c00053
Acc. Mater. Res. 2021, 2, 7−20

are not evident (Figure 5h).[10] The effectiveness of manipulating graphene sheet alignment through a step-expansion flow is thus further confirmed. In comparison, a gradual-expansion GO flow formed by reversing the flow direction in the contracted microchannel does not yield highly aligned GO sheets. The extension rate of the gradual-expansion flow, which is 3 orders of magnitude lower than the highest extension rate in the step-expansion flow, results in randomly oriented GO sheets at the microchannel outlet.[6]

4. HIGH TEMPERATURE THERMAL ANNEALING

High temperature heat treatment above 2000 °C under an inert atmosphere is practiced during the production of conventional PAN- and MPP-based CFs.[10,25,31,32] On the microscale, the crystallite dimension in the direction parallel to the fiber axis of both types of CFs increases monotonically as the heat treatment temperature increases from 1300 °C up to 2700 °C.[10] On the nanoscale, for PAN-based CFs in particular, high temperature induces new C−C bonding during the removal of nitrogen atoms.[33] While both types of CFs exhibit outstanding Young's modulus and tensile strength, PAN-based CFs display higher tensile strength due to abundant C−C cross-links, and MPP-based CFs have higher Young's moduli but lower tensile strength due to their larger crystalline dimensions.[10]

In addition to increasing Young's modulus, the growth of crystallite domains in CFs also contributes to the increase of thermal and electrical conductivities. Since the size of crystallites in MPP-based CFs are generally larger, their conductivities are usually higher. However, both PAN- and MPP-based CFs suffer from relatively low electrical and thermal conductivities for a number of factors. In PAN-based CFs, sp^3 hybridized cross-linking atoms behave as phonon scattering centers and disrupt delocalized π-bonds, limiting both thermal and electrical conductivities.[5,10,11] While for MPP-based CFs, despite having larger crystallite sizes than PAN-based CFs, the growth of crystallites is still somewhat hindered by the formation of hydrogen bonding between adjacent carbonyl and carboxyl groups during the necessary oxidation process prior to carbonization.[34]

In 2013, GO heat treatment experiments by Song et al. revealed that, at a high temperature of 2000 °C, GO sheets were reorganized into a highly ordered hexagonal carbon lattice structure.[35] The morphology of this annealed graphene material, with its isolated carbon sheets, resembled that of high temperature treated carbon materials, such as CFs. Moreover, X-ray photoelectron spectroscopy (XPS) showed that all oxygen-containing functional groups were removed from the carbon lattice structure. These striking similarities of the effect of high temperature thermal treatment between GO and conventional CFs, with highly conductive MPP-based CFs in particular, raise the question of what effects high temperature thermal treatment would have on GFs and other graphene-based assemblies with GO sheets as precursors.

4.1. Limitations of Chemical Reduction and Mild Temperature Thermal Annealing

In the earlier research of GFs, up to 2015, chemical reduction and thermal annealing at mild temperatures (800−1500 °C) were the common approaches taken to enhance the mechanical properties and electrical conductivities of GFs.[22,36,37] Both approaches result in the removal of the majority of oxygen-containing functional groups, leading to a decrease in interlayer distance and an increase in sp^2 carbon atoms. The decrease in interlayer distance allows for stronger van der Waals interactions between graphene sheets and strengthens the hydrogen bonding between residual oxygen-containing functional groups.[5] The combined effect leads to an increase in tensile strength and Young's modulus. The increase in sp^2 carbon atoms allows for the formation of a delocalized π cloud, enhancing the electrical conductivity of GFs.[11] However, despite the attributes of these two approaches, the tensile strength (100−900 MPa) and Young's modulus (5−20 GPa) of these GFs are still one magnitude lower than that of CFs.[22,36,37] The electrical conductivities of these GFs are also consistently limited to $<10^5$ S m^{-1}, lower than that of CNT fibers.[26]

The limitations of chemical reduction that prevents further improvements in GF performance include the inability to fully remove oxygen-containing functional groups, the introduction of microvoids during the removal of oxygen-containing functional groups as gaseous H_2O, and the inability to increase crystallite size and improve crystallite orientation through the rearrangement of the turbostratic graphite microstructure.[5] Compared to chemical reduction, mild temperature thermal annealing will lead to an increase in GF crystallinity.[7] However, the thermal annealing process releases CO_2 and CO in addition to H_2O.[5] This results in the formation of more microvoids at mild annealing temperatures and a reduced GF compactness due to carbon loss, balancing out the benefits of a higher crystallinity to GF performance.[5]

4.2. Superior Performances of High Temperature Annealed GFs

Driven by the aforementioned successful conversion of random GO sheets into a graphitic structure through high temperature thermal annealing, and in order to improve GF performance beyond the limitations of chemical and mild temperature thermal reduction, our group applied high temperature thermal annealing (up to 2850 °C) to GF fabrication in 2015.[5] In combination with the strategy of optimizing the ratio of GGO and SGO, the high temperature thermally annealed GFs achieved significant and simultaneous improvements in tensile strength, Young's modulus, and electrical conductivity. Notably, the reported thermal conductivity was higher than the highest thermal conductivity reported in CFs.[38]

More recently, in combination with employing high aspect ratio flat microchannels for wet-spinning, graphene belts thermally annealed at 2500 °C further achieved excellence in their mechanical, electrical, and thermal performances. Measured using an electromechanical test system with a 20 mm gauge length and 0.5 mm min^{-1} extension rate, the tensile strength of these graphene belts reached 1.9 GPa, and their Young's moduli reached 309 GPa. The electrical conductivity of these graphene belts measured by a four-probe method exceeds that of all conventional CFs at 1.0×10^6 S m^{-1}, while their thermal conductivity of 1575 W m^{-1} K^{-1} measured by a well-established electrical self-heating method surpasses that of all macroscale graphene-based assemblies.[6]

Aside from our group's efforts, Xu et al. further pushed the limit of the thermal annealing temperature to 3000 °C.[7] The average tensile strength and Young's modulus measured at 5 mm gauge, and electrical conductivity of the GGO GFs are 1.78 GPa, 385 GPa, and 8×10^5 S m^{-1}, respectively. More recently, Li et al. developed a continuous plasticization stretching method that regulates the intrinsic wrinkling of

https://dx.doi.org/10.1021/accountsmr.0c00053
Acc. Mater. Res. 2021, 2, 7−20

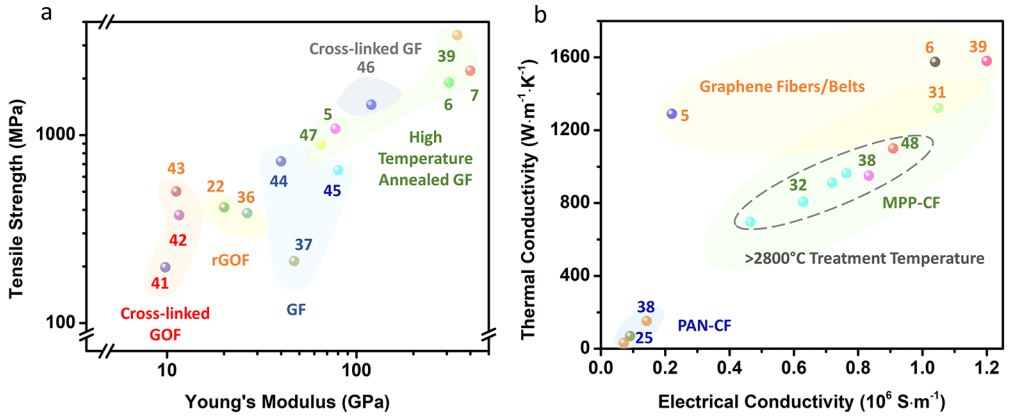

Figure 6. State-of-the-art mechanical properties and transport behavior of carbonaceous fiber structures: (a) tensile strength and Young's modulus of high temperature annealed GFs and comparison with previously reported GFs, GOFs, and rGO fibers; (b) comparison of thermal conductivity and electrical conductivity of high temperature annealed graphene fibers/belts with MPP-based CFs and PAN-based CFs.

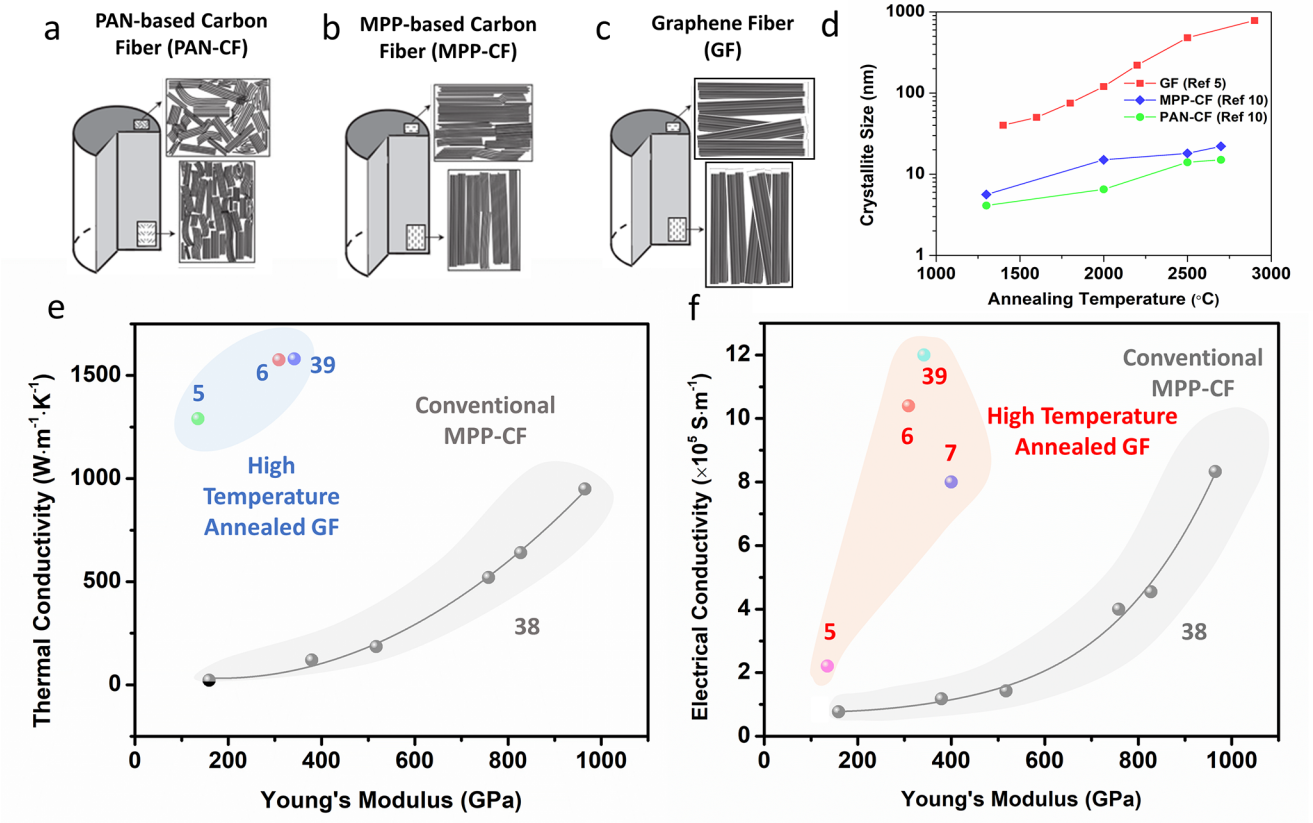

Figure 7. Correlations of Young's modulus with thermal and electrical conductivities of graphene-based macroscopic structures: (a)−(c) sketches of the structural rearrangement and size of the graphitic domains in PAN-based CFs, MPP-based CFs, and high temperature annealed GFs (reproduced with permission from ref 10; copyright 2012 Elsevier); (d) crystallite sizes as a function of annealing temperature; (e, f) thermal and electrical conductivity deviations of the macroscopic graphene structures from conventional CFs.

GO sheets in GOFs.[39] By intercalation of GO with small molecule plasticizers, the interlayer distance increases from 1.0 to 1.2−1.8 nm, resulting in a decrease in the van der Waals attraction between adjacent graphene sheets. Under tension, the lower van der Waals attraction leads to plastic interlayer sliding instead of elastic deformation. Within the interlayer distance range 1.2−1.8 nm, the interlayer attraction and sliding are in balance. Large plastic deformations of GO sheets occur and result in the flattening of wrinkles. With the elimination of their wrinkles, GO sheets become more compact and aligned. The extended conformation of straightened GO sheets also facilitates substantial growth of the graphitic crystallites along the stretching direction during high temperature thermal annealing. Both these effects lead to a new record mechanical strength of 3.4 GPa in their GFs. Meanwhile, focusing on a substantial reduction in annealing time, Noh et al. successfully developed a Joule heating method using a high electrical current to anneal GOFs at temperatures up to 2000 °C.[40] Within only 5 min, the sp^2 lattice structure was largely restored within the fibers. Despite lower than that of GFs annealed

https://dx.doi.org/10.1021/accountsmr.0c00053
Acc. Mater. Res. 2021, 2, 7−20

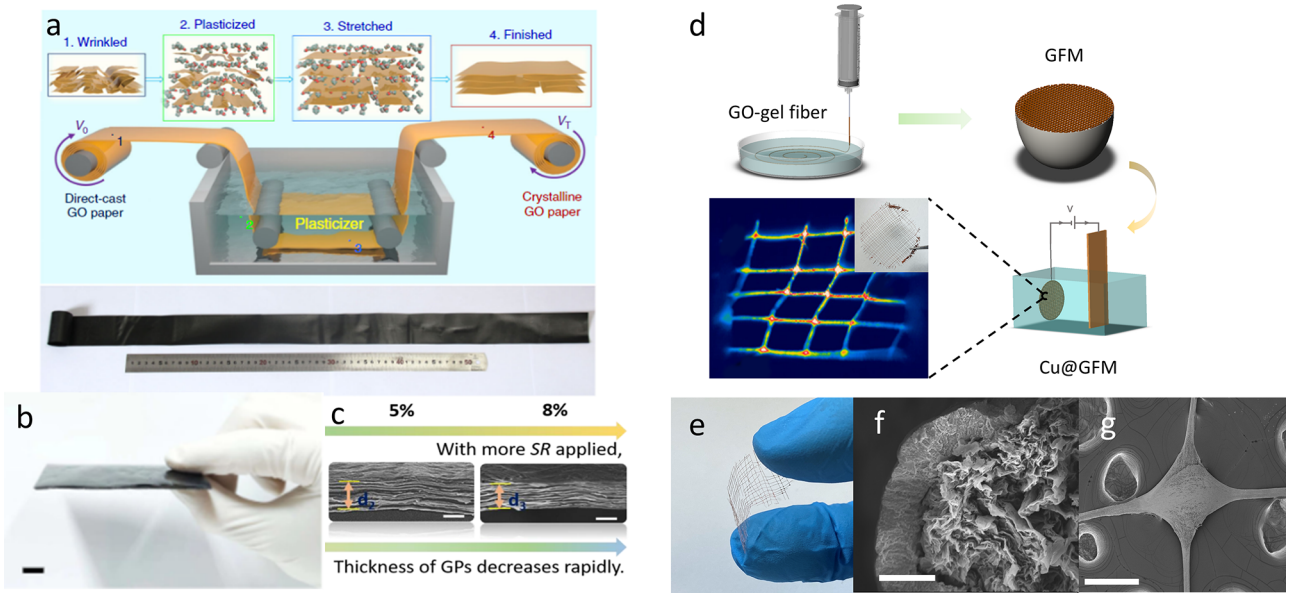

Figure 8. Scalable manufacturing of macroscopic 2D graphene structures (reproduced with permission from ref 54; copyright 2020 Springer Nature) and the assembly of the 3D flexible GF-composite meshes (reproduced with permission from ref 49; copyright 2020 American Chemical Society): (a) production of highly crystalline GPs by a plasticization stretching method; (b) laminated composites consisting of GPs; (c) thickness of GPs at different stretching rates (scale bar, 2 μm); (d) production of Cu-coated GFMs; (f) a uniform copper coating on individual GFs; (g) a fused intersection within a Cu-coated GFM. Scale bars, 10mm (b), 2 μm (c), 2μm (f) and 100μm (g).

conventionally in furnaces over an extended time, the electrical conductivity of these fibers reached ~1.0×10^6 S m^{-1}. This result of electric current annealing demonstrates the promise and inspires the adoption of more environmentally benign and energy-efficient ways to improve GF performance.

Overall, high temperature annealing has allowed GFs and their fiber-like derivatives, such as graphene belts, to far outperform GFs annealed at milder temperatures and other forms of graphene-based fibers in mechanical performance. Only cross-linked GFs can reach the same magnitude of tensile strength and Young's modulus, usually at the expense of their electrical and thermal conductivities (Figure 6a).[5−7,22,41−47] In comparison to conventional CFs, high temperature annealed GFs are capable of achieving higher thermal and electrical properties even with significantly lower Young's moduli. This deviates from the traditional wisdom that high conductivities always correlate with an ultrahigh stiffness (Figure 6b).[5,6,25,31,32,38,39,48] The increased flexibility of high temperature annealed GFs is favorable for applications where the stiffness of conventional MPP CFs is not desired, for example, in wearable electronics.

4.3. Crystallographic and Chemical Effects of High Temperature Annealing on GFs

The chemical and crystallographic evolution of GF microstructure during high temperature annealing ultimately dictates the performance of GFs. Microstructure evolution during high temperature annealing has multiple impacts on the mechanical, electrical, and thermal performances of GFs. The most profound impact is arguably causing the trends where Young's modulus and the electrical and thermal conductivities increase monotonically with the increase of annealing temperatures. On the one hand, these trends can be attributed to the monotonic growth of crystallite size in GFs with the rise of annealing temperatures. This is consistent with the effect of thermal annealing on CFs and supported by the increase of I_G/I_D shown by the Raman spectra of GFs when the annealing temperatures increase from 1400 to 2850 °C.[5,38] On the other hand, the monotonic increase of electrical and thermal conductivities can be explained by the lowering of the impedance of electron transport and the decrease in phonon scattering points by reducing the number of sp^3 carbon atoms and grain boundaries.[5,11,25] As thermal annealing temperatures increase, the removal of oxygen-containing functional groups prompts the transformation of sp^3 carbon into sp^2 carbon. This transformation, also supported by the increase of I_G/I_D, allows for more phonon transport through sp^2 bonding networks, enhancing thermal conduction.[5] In the meantime, more sp^2 bonding translates to a more favorable condition for delocalized π-bonding formation, which also facilitates electrical conduction.[11] As for decreasing electron impedance and phonon scattering at grain boundaries, high temperature thermal annealing is also beneficial due to the growth of crystallite size and the corresponding decrease of the number of grain boundaries. Compared to the crystallite size of conventional CFs, the crystallite size of high temperature thermal annealed GFs is much larger, contributing greatly to its superior conductivities (Figure 7).[5−7,38,39]

In contrast to the hindering effect of sp^3 carbon atoms on thermal and electrical conductivities, C−C cross-links between graphene sheets are crucial to the tensile strength of GFs. Together with graphene sheet alignment and compactness, these cross-links determine the tensile strength of GFs. As annealing temperatures increase but remain below 1800 °C, the increase in tensile strength can be mainly attributed to densification and the enhancement of alignment of graphene sheets. At these lower temperatures, substantial oxygen-containing functional groups still remain even though some decomposition occurs during annealing. Hydrogen bonds between these remaining oxygen-containing functional groups are thus maintained. New cross-links between adjacent graphene sheets may also be formed during the decomposition of oxygen-containing functional groups.[5] These cross-links and

https://dx.doi.org/10.1021/accountsmr.0c00053
Acc. Mater. Res. 2021, 2, 7−20

the hydrogen bonds between functional groups have a similar effect of opposing graphene sheets from gliding.[10] The concerted effect of improved graphene sheet alignment and compactness, and the abundance of cross-links allows the tensile strength of GFs to peak when treated at 1800 °C. Increasing thermal annealing temperatures from 1800 to 2000 °C leads to the slowing down of the improvement of graphene sheet alignment and compactness while accelerating the removal of cross-links. As a result, a substantial drop occurs in GF tensile strength. At 2000 °C, all cross-links are fully removed. The GF tensile strength remains constant as annealing temperatures further increase.[5]

5. UNIQUE MICROSTRUCTURE CONTROL METHODS FOR GRAPHENE PAPERS AND GRAPHENE FIBER MESHES

Discussed in the previous section, the effect of the crystallographic and chemical evolution on GF performance also holds true for the performance of other graphene-based assemblies, including GPs and GFMs (Figure 8).[9,49] As one of the earliest macroscale graphene assemblies, GPs were first developed as a cost-effective alternative to graphite films fabricated through the pyrolysis of aromatic polyimide films and bucky papers fabricated from carbon nanotubes. Similar to their competitors, GPs have been widely applied to research projects in thermal management, electromagnetic interference (EMI) shielding, and supercapacitor development.[9,50,51] Due to the requirements of these applications, it has been essential for GPs to simultaneously possess high mechanical strength and electrical and thermal conductivities to stand out among their competitors.

Compared to GPs, GFMs are newcomers to the family of macroscale graphene-based assemblies. As a 2D derivative of GFs, GFMs have shown great applicational potentials in thermal management, EMI shielding, and energy storage applications.[49,52] However, in contrast to GPs, mechanical strengthening is not of high importance for GFMs. Conversely, one of their most important attributes is achieving flexibility while retaining excellent electrical and thermal conductivities.[49]

5.1. Unique Methods for Improving Graphene Sheet Alignment and Densification in GPs

Similar to the poststretching strategy employed by Xu et al. on GFs for the mechanical realignment of graphene sheets,[7] the graphene sheet alignment in graphene papers can also be improved by mechanical pressing. In 2014, our group demonstrated that by applying mechanical pressing to electrospray deposited GPs before thermal annealing, graphene sheets in the GPs can be well-aligned and stacked, showing a highly ordered microstructure.[9] After mechanical pressing, the density of these GPs without thermal annealing increased from 0.35 to ~2.0 g cm^{-3}. The electrical and thermal conductivities are improved greatly from 2175 S m^{-1} and 20.7 W m^{-1} K^{-1} to 17214 S m^{-1} and 173 W m^{-1} K^{-1}. Other identified factors that impact the graphene sheet alignment in GPs fabricated by direct electrospray deposition include solution concentration, flow rate, and electric potential between the deposition nozzle and substrate. Combined with high temperature thermal annealing at 2850 °C, electrical and thermal conductivities of GPs reach 1.83×10^5 S m^{-1} and 1434 W m^{-1} K^{-1}.[9] In 2017, our group further identified that slow flow rates and low solution concentrations were beneficial for obtaining an ordered and aligned graphene assembly in GPs fabricated by electrospray deposition.[53] At low concentrations, graphene sheets can fully disperse within each droplet; while at a low flow rate, fine droplets can be formed, allowing for an even deposition over a substrate. Well-dispersed graphene sheets deposited in fine droplets stack up more easily in an ordered layer-by-layer structure via van der Waals force, resulting in enhanced compactness, electrical conductivity, and thermal conductivity of GPs.[9]

Besides enhancing the electrical and thermal properties, GPs can also be mechanically strengthened by improving graphene sheet alignment. Using the same continuous plasticization stretching method as for their outstanding GFs, Li et al. regulated the intrinsic wrinkling of GO sheets in GO papers (GOPs) (Figure 8a–c).[54] Stacking disorders caused by this wrinkling, including crumbles, folds, and dislocations, were significantly relieved. These improvements in the microstructure of GPs resulted in a high tensile strength of 1.1 GPa being reported.

5.2. Wet-Fusing Technique for Forming Flexible yet Conductive GFMs

Many advanced CF applications involve making CFs into carbon fiber fabrics. However, electrical and thermal conductivities are not strong suits of the CF fabrics,[55] limiting their functional applications. Also, due to their high stiffness, weaving CFs is difficult and forming strong interactions between fibers is even more challenging.[56,57] Compared to bonding in CFs, direct interfiber bonding between GFs can be established by the wet-fusing assembly, forming the basis for fabricating electrically and thermally conductive nonwoven GF fabrics.[58]

When redispersed into an aqueous solvent, dried GOFs are immediately wetted. These wetted fibers gradually swell into GO gel fibers. Crossing one GO gel fiber with another and evaporating the solvent through natural drying fuses two GO gel fibers to each other due to hydrogen bonding forming between the GO sheets at the fiber interfaces. By fusing a large amount of short GO gel fibers together and annealing the macroscale fused fiber structure at high temperatures (>1000 °C), Li et al. obtained the first nonwoven GF fabric.[58]

On the basis of the principle of wet-fusing assembly, our group reported that GO gel fibers directly coagulated in a dimethylformamide-based solution could directly fuse together when taking two fibers out of the coagulation bath and crossing one over the other.[49] This wet-fusing of GOFs outside of a liquid solution allows for neat orthogonal GFMs (Figure 8d–g) to be fabricated with longer individual GO gel fibers. Due to hydrogen bonding-induced random reorganization of GO sheets, the fused junctions serve as electron impeding and phonon scattering locations. With longer GO gel fibers and a grid layout, the number of fused junctions decreases while GFMs observe higher electrical and thermal conductivities, despite only being thermally reduced at a modest temperature of 1000 °C. Their relatively high electrical conductivity allows a thin layer of copper to be electroplated onto GFMs (Figure 8d), further enhancing the electrical conductivity. However, despite their partial obstruction of electron and phonon transports, the random alignment of graphene sheets within fused junctions gives a more flexible character to GFMs (Figure 8e). We speculate adding tension to the GO gel fibers during interfusing or thermal annealing might increase the degree of alignment of GO sheets in the fused junctions.

https://dx.doi.org/10.1021/accountsmr.0c00053
Acc. Mater. Res. 2021, 2, 7–20

However, more investigation is needed on whether this or other microstructure enhancing techniques used for GFs or GPs would be useful to improve the graphene sheet alignment or crystallinity at fused intersections. It would also be intriguing to see how these improvements would benefit the performance of GFMs. As for now, their unique mechanical properties and excellent electrical and thermal conductivities of GFMs and other wet-fusing derived GF fabrics have fostered a variety of promising applications, including thermal management, EMI shielding, and energy storage.[49,52,58]

6. CONCLUSION AND OUTLOOK

A little more than a decade since the discovery of the first macroscale graphene-based assemblies, a vibrant field of research yielding a wide variety of assemblies with several generations of iterations has been opened up with the dedication of numerous research groups. Multiple methods have been developed to optimize the microstructures of graphene-based assemblies and explore their potential applications in a wider range of technological arenas (Figure 8). With the advancements of assembly approaches and optimized microstructures, we have witnessed a significant improvement in the mechanical, electrical, and thermal performances of these assemblies.

Microstructures of graphene-based assemblies have an intertwining multiscale effect on their performance. Nanoscale cross-links between adjacent graphene sheets enhance tensile strength yet introduce electron impeding and phonon scattering points, hindering electrical and thermal conductance. Improved sheet alignment leads to improved Young's modulus. Crystallite growth contributes to enhance both Young's modulus and conductivities. Densification, interestingly, is a way to enhance all the three main aspects of mesoscale graphene-based assembly performance. Since 2014, our group has been at the forefront in developing graphene-based macroscopic structures and optimizing their properties and performance.[9] Strategies, including using a mixture of large and small GO sheets as the precursor, constraining GO flow during wet-spinning to a flat microchannel, and thermally annealing GFs to temperatures above 1500 °C, are developed to comprehensively manipulate the microstructures of GFs and improve their overall performance. A better understanding is achieved on the close correlation among the assembly process, assembly microstructure, and the performance of the assembly. With this understanding, new methods have also been adapted for the fabrication of GPs and GFMs with their unique microstructures and performance characteristics.

With the research efforts of our group and many others, the direct fabrication of functional carbon materials from 2D graphene sheets with well-maintained properties has become much more realistic. Currently, the highest reported electrical and thermal conductivities of both GPs and GFs have far exceeded those of PAN- and MPP-based CFs (Figure 9).[6,39,54] Substantial improvement in the mechanical properties of GFs has also taken place since their inception. The highest reported tensile strength of GFs is on par with that of high-performance MPP-based CFs while being significantly more flexible (Figure 9).[39] However, given that there is still a large performance gap between graphene-based assemblies and their theoretical potentials, new enhancement efforts are still in demand, especially for further increasing mechanical strength. Some potentially promising mechanical strengthening methods include further enhancing compactness,[12] magnetically enhancing GO alignment,[59] simultaneous stretching and high temperature annealing,[60] and GO plasticization.[39,54]

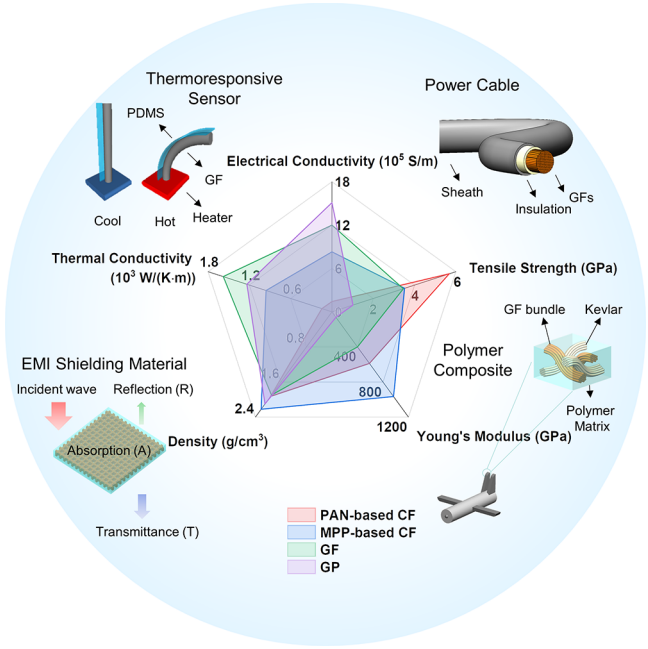

Figure 9. State-of-the-art performances and functionalities of graphene-based macroscopic assemblies and their potential technological applications in thermoresponsive sensors, power cables, EMI shielding materials, and strong and highly conductive polymer composites.

Recognizing the intrinsic limits in further improving the mechanical properties of monolithic graphene macroscopic assemblies, multiple interfacial cross-linking strategies, e.g., $\pi-\pi$ bonding, ionic bonding, and hydrogen bonding, have been applied for the synergetic enhancement of the mechanical and even electrical properties of GFs and GPs. Long-chain $\pi-\pi$ bonding, in particular, provides large movement space for graphene sheets allowing for excellent stress dissipation and even better resilience to cyclic stretching.[20] Similarly, ionic bonding can be used to increase interaction between neighboring graphene sheets, e.g., Cr^{3+} or Ca^{2+} is used to form ionic bonds on both sides with oxygen-containing functional groups on the edge of neighboring rGO sheets.[18,21] Graphene sheets in GPs cross-linked by $\pi-\pi$ bonding show a higher degree of alignment and resistance to shear deformation under cyclic stretching than those cross-linked by ionic bonding.[18] Compared to van der Waals bonding, hydrogen bonding can withstand larger strain rates. By interconnecting the partially oxidized edges of different graphene sheets through hydrogen bonding, e.g., using the hydroxyl-containing nanofibers,[61] the interaction between neighboring graphene sheets becomes stronger, significantly increasing the load resistance of the composite. Compared to $\pi-\pi$ bonding, covalent bonding is generally stronger but shorter in range. It has been successfully introduced to cross-link graphene sheets to black phosphorus nanosheets.[16] Black phosphorus nanosheets can slide more easily against each other compared to graphene sheets, causing plastic deformation in the macrostructure and an increase in the toughness of the macrostructure. While interfacial bonding is an important approach to further improve the mechanical properties of the macroscopic graphene structures to be commensurate with that of

https://dx.doi.org/10.1021/accountsmr.0c00053
Acc. Mater. Res. 2021, 2, 7−20

their carbon fiber counterparts, the addition of ionic or hydrogen bonding will inevitably reduce electron and thermal transport. Within the context of simultaneous enhancement of electrical, thermal and mechanical properties, $\pi-\pi$ bonding is much more desirable as $\pi-\pi$ bonding interacts with the basal plane of the graphene sheets without disturbing their sp^2-conjugated structures.[18]

Besides further enhancing the performance of 1D GFs and 2D GPs and GFMs, the development of high-performance 3D graphene-based assemblies using established microstructure enhancement strategies also deserves further attention. Currently, 3D graphene-based assemblies consist of a large variety of hydrogels, foams, and aerogels. Due to their high surface to volume ratios and lower than air density, graphene aerogels (GAs) have been a focus of intense research on energy storage, biomedicine, and catalyst engineering.[3] GAs are prepared by the freeze or supercritical drying of GO sol–gels, followed by a chemical or thermal reduction process. During the freeze-drying process, it has been found that the majority of GO sheets preferentially align along the direction of ice crystal growth. This finding has lead to the improvements of compressive strength and electrical conductivity in GAs by unidirectional and bidirectional freezing.[62,63] However, despite these signs of progress, 3D graphene-based assemblies, with the example of GAs, still lag far behind 1D and 2D assemblies in electrical and thermal conductivities and exhibit insufficient tensile strength.[63] In the short term, an intriguing topic would be to investigate how to further improve the alignment of graphene sheets and the orientation of graphitic crystallites in 3D graphene-based assemblies, such as GAs. Understanding how these microstructural alterations will impact the mechanical, electrical, and thermal properties in 3D assemblies is also of high importance. Such further efforts will help broaden the application of graphene-based assemblies and their composites as flexible sensors and antennae, flexible and lightweight power cables, EMI shielding textiles, and strong and highly conductive polymer composites for advanced multifunctional applications (Figure 9).

AUTHOR INFORMATION

Corresponding Author

Jie Lian − *Department of Mechanical, Aerospace and Nuclear Engineering, Rensselaer Polytechnic Institute, Troy, New York 12180, United States;* orcid.org/0000-0002-9060-8831; Email: lianj@rpi.edu

Author

Mingxin Li − *Department of Mechanical, Aerospace and Nuclear Engineering, Rensselaer Polytechnic Institute, Troy, New York 12180, United States;* orcid.org/0000-0003-3276-9140

Complete contact information is available at: https://pubs.acs.org/10.1021/accountsmr.0c00053

Notes

The authors declare no competing financial interest.

Biographies

Mingxin Li obtained his B.S. degree from Beijing Institute of Technology in 2017. He is currently a Ph.D. student in Prof. Lian's Nanonuclear and Energy Materials Group at Rensselaer Polytechnic Institute. His general research interest is in the development of functional composite materials based on graphene fibers and their related graphene-based assemblies.

Jie Lian obtained his Ph.D. degree from University of Michigan in 2003 and is currently a Professor in the Department of Mechanical, Aerospace and Nuclear Engineering, Rensselaer Polytechnic Institute. His research interests mainly focus on fundamental materials behavior under extreme environments, nanoscale design for developing advanced materials with enhanced performance, novel nanostructured materials for alternative energy applications, and nanoassembly and synthesis science of advanced materials, including 2D perovskite, graphene, and their applications.

ACKNOWLEDGMENTS

This work was financially supported by the US National Science Foundation under the award of DMR 1742806.

REFERENCES

(1) Xu, Z.; Gao, C. Graphene Chiral Liquid Crystals and Macroscopic Assembled Fibres. *Nat. Commun.* **2011**, *2*, 571.

(2) Chen, H.; Müller, M. B.; Gilmore, K. J.; Wallace, G. G.; Li, D. Mechanically Strong, Electrically Conductive, and Biocompatible Graphene Paper. *Adv. Mater.* **2008**, *20*, 3557–3561.

(3) Gorgolis, G.; Galiotis, C. Graphene aerogels: a review. *2D Mater.* **2017**, *4*, 032001.

(4) Xu, Z.; Gao, C. Graphene in Macroscopic Order: Liquid Crystals and Wet-Spun Fibers. *Acc. Chem. Res.* **2014**, *47*, 1267–1276.

(5) Xin, G.; Yao, T.; Sun, H.; Scott, S. M.; Shao, D.; Wang, G.; Lian, J. Highly Thermally Conductive and Mechanically Strong Graphene Fibers. *Science* **2015**, *349*, 1083–1087.

(6) Xin, G.; Zhu, W.; Deng, Y.; Cheng, J.; Zhang, L. T.; Chung, A. J.; Suvranu, D.; Lian, J. Microfluidics-Enabled Orientation and Microstructure Control of Macroscopic Graphene Fibres. *Nat. Nanotechnol.* **2019**, *14*, 168–175.

(7) Xu, Z.; Liu, Y.; Zhao, X.; Peng, L.; Sun, H.; Ren, X.; Jin, C.; Xu, P.; Wang, M.; Gao, C. Ultrastiff and Strong Graphene Fibers via Full-Scale Synergetic Defect Engineering. *Adv. Mater.* **2016**, *28*, 6449–6456.

(8) Dong, Z.; Jiang, C.; Cheng, H.; Zhao, Y.; Shi, G.; Jiang, L.; Qu, L. Facile Fabrication of Light, Flexible and Multifunctional Graphene Fibers. *Adv. Mater.* **2012**, *24*, 1856–1861.

(9) Xin, G.; Sun, H.; Hu, T.; Fard, H. R.; Sun, X.; Koratkar, N.; Borca-Tasciuc, T.; Lian, J. Large-Area Freestanding Graphene Paper for Superior Thermal Management. *Adv. Mater.* **2014**, *26*, 4521–4526.

(10) Qin, X.; Lu, Y.; Xiao, H.; Wen, Y.; Yu, T. A Comparison of the Effect of Graphitization on Microstructures and Properties of Polyacrylonitrile and Mesophase Pitch-Based Carbon Fibers. *Carbon* **2012**, *50*, 4459–4469.

(11) Sreeprasad, T. S.; Berry, V. How Do the Electrical Properties of Graphene Change with Its Functionalization? *Small* **2013**, *9*, 341–350.

(12) Mao, L.; Park, H.; Soler-Crespo, R. A.; Espinosa, H. D.; Han, T. H.; Nguyen, S. T.; Huang, J. Stiffening of graphene oxide films by soft porous sheets. *Nat. Commun.* **2019**, *10*, 3677.

(13) Akbari, A.; Cunning, B. V.; Joshi, S. R.; Wang, C.; Camacho-Mojica, D. C.; Chatterjee, S.; Modepalli, V.; Cahoon, C.; Bielawski, C. W.; Bakharev, P.; Kim, G. H.; Ruoff, R. S. Highly Ordered and Dense Thermally Conductive Graphitic Films from a Graphene Oxide/Reduced Graphene Oxide Mixture. *Matter* **2020**, *2*, 1198–1206.

(14) Wan, S.; Li, Y.; Peng, J.; Hu, H.; Cheng, Q.; Jiang, L. Synergistic toughening of graphene oxide–molybdenum disulfide–thermoplastic polyurethane ternary artificial nacre. *ACS Nano* **2015**, *9*, 708–714.

(15) Wan, S.; Zhang, Q.; Zhou, X.; Li, D.; Ji, B.; Jiang, L.; Cheng, Q. Fatigue resistant bioinspired composite from synergistic two-dimensional nanocomponents. *ACS Nano* **2017**, *11*, 7074–7083.

(16) Zhou, T.; Ni, H.; Wang, Y.; Wu, C.; Zhang, H.; Zhang, J.; Tomsia, A. P.; Jiang, L.; Cheng, Q. Ultratough graphene−black phosphorus films. *Proc. Natl. Acad. Sci. U. S. A.* **2020**, *117*, 8727−8735.
(17) Zhou, T.; Wu, C.; Wang, Y.; Tomsia, A. P.; Li, M.; Saiz, E.; Fang, S.; Baughman, R. H.; Jiang, L.; Cheng, Q. Super-tough MXene-functionalized graphene sheets. *Nat. Commun.* **2020**, *11*, 2077.
(18) Wan, S.; Fang, S.; Jiang, L.; Cheng, Q.; Baughman, R. H. Strong, conductive, foldable graphene sheets by sequential ionic and π bridging. *Adv. Mater.* **2018**, *30*, 1802733.
(19) Wan, S.; Li, Y.; Mu, J.; Aliev, A. E.; Fang, S.; Kotov, N. A.; Jiang, L.; Cheng, Q.; Baughman, R. H. Sequentially bridged graphene sheets with high strength, toughness, and electrical conductivity. *Proc. Natl. Acad. Sci. U. S. A.* **2018**, *115*, 5359−5364.
(20) Wan, S.; Chen, Y.; Wang, Y.; Li, G.; Wang, G.; Liu, L.; Zhang, J.; Liu, Y.; Xu, Z.; Tomsia, A. P.; Jiang, L. Ultrastrong graphene films via long-chain π-bridging. *Matter* **2019**, *1*, 389−401.
(21) Park, H.; Lee, K. H.; Kim, Y. B.; Ambade, S. B.; Noh, S. H.; Eom, W.; Hwang, J. Y.; Lee, W. J.; Huang, J.; Han, T. H. Dynamic assembly of liquid crystalline graphene oxide gel fibers for ion transport. *Sci. Adv.* **2018**, *4*, No. eaau2104.
(22) Xu, Z.; Sun, H.; Zhao, X.; Gao, C. Ultrastrong Fibers Assembled from Giant Graphene Oxide Sheets. *Adv. Mater.* **2013**, *25*, 188−193.
(23) Zhang, Y.; Zheng, L.; Sun, G.; Zhan, Z.; Liao, K. Failure Mechanisms of Carbon Nanotube Fibers under Different Strain Rates. *Carbon* **2012**, *50*, 2887−2893.
(24) Koziol, K.; Vilatela, J.; Moisala, A.; Motta, M.; Cunniff, P.; Sennett, M.; Windle, A. High-Performance Carbon Nanotube Fiber. *Science* **2007**, *318*, 1892−1895.
(25) Qiu, L.; Zheng, X. H.; Zhu, J.; Su, G. P.; Tang, D. W. The Effect of Grain Size on the Lattice Thermal Conductivity of an Individual Polyacrylonitrile-Based Carbon Fiber. *Carbon* **2013**, *51*, 265−273.
(26) Behabtu, N.; Young, C. C.; Tsentalovich, D. E.; Kleinerman, O.; Wang, X.; Ma, A. W.; Bengio, E. A.; ter Waarbeek, R. F.; de Jong, J. J.; Hoogerwerf, R. E.; Fairfield, S. B.; Ferguson, S. B.; Maruyama, B.; Kono, J.; Talmon, Y.; Cohen, Y.; Otto, M. J.; Pasquali, M. Strong, Light, Multifunctional Fibers of Carbon Nanotubes with Ultrahigh Conductivity. *Science* **2013**, *339*, 182−186.
(27) Pathipati, S. R. Electronic Transport Properties of Graphene and Graphene-Related Materials. *Doctoral dissertation*, University of Nova Gorica, Nova Gorica, Slovenia, 2014.
(28) Kiriya, D.; Kawano, R.; Onoe, H.; Takeuchi, S. Microfluidic Control of the Internal Morphology in Nanofiber-Based Macroscopic Cables. *Angew. Chem.* **2012**, *124*, 8066−8071.
(29) Trebbin, M.; Steinhauser, D.; Perlich, J.; Buffet, A.; Roth, S. V.; Zimmermann, W.; Thiele, J.; Förster, S. Anisotropic Particles Align Perpendicular to the Flow Direction in Narrow Microchannels. *Proc. Natl. Acad. Sci. U. S. A.* **2013**, *110*, 6706−6711.
(30) Schlenk, M.; Hofmann, E.; Seibt, S.; Rosenfeldt, S.; Schrack, L.; Drechsler, M.; Rothkirch, A.; Ohm, W.; Breu, J.; Gekle, S.; Förster, S. Parallel and Perpendicular Alignment of Anisotropic Particles in Free Liquid Microjets and Emerging Microdroplets. *Langmuir* **2018**, *34*, 4843−4851.
(31) Zhang, X.; Ning, S.; Ma, Z.; Song, H.; Wang, D.; Zhang, M.; Fan, B.; Zhang, S.; Yan, X. The structural properties of chemically derived graphene nanosheets/mesophase pitch-based composite carbon fibers with high conductivities. *Carbon* **2020**, *156*, 499−505.
(32) Guo, J.; Li, X.; Xu, H.; Zhu, H.; Li, B.; Westwood, A. Molecular Structure Control in Mesophase Pitch via Co-Carbonization of Coal Tar Pitch and Petroleum Pitch for Production of Carbon Fibers with Both High Mechanical Properties and Thermal Conductivity. *Energy Fuels* **2020**, *34*, 6474−6482.
(33) Huang, X. Fabrication and Properties of Carbon Fibers. *Materials* **2009**, *2*, 2369−2403.
(34) Chung, D. L. *Carbon Fiber Composites*. Butterworth-Heinemann: Boston, 1994; pp 3−65.
(35) Song, L.; Khoerunnisa, F.; Gao, W.; Dou, W.; Hayashi, T.; Kaneko, K.; Endo, M.; Ajayan, P. M. Effect of High-Temperature Thermal Treatment on the Structure and Adsorption Properties of Reduced Graphene Oxide. *Carbon* **2013**, *52*, 608−612.
(36) Tian, Q.; Xu, Z.; Liu, Y.; Fang, B.; Peng, L.; Xi, J.; Li, Z.; Gao, C. Dry Spinning Approach to Continuous Graphene Fibers with High Toughness. *Nanoscale* **2017**, *9*, 12335−12342.
(37) Xiang, C.; Young, C. C.; Wang, X.; Yan, Z.; Hwang, C. C.; Cerioti, G.; Lin, J.; Kono, J.; Pasquali, M.; Tour, J. M. Large Flake Graphene Oxide Fibers with Unconventional 100% Knot Efficiency and Highly Aligned Small Flake Graphene Oxide Fibers. *Adv. Mater.* **2013**, *25*, 4592−4597.
(38) Emmerich, F. G. Young's Modulus, Thermal Conductivity, Electrical Resistivity and Coefficient of Thermal Expansion of Mesophase Pitch-Based Carbon Fibers. *Carbon* **2014**, *79*, 274−293.
(39) Li, P.; Liu, Y.; Shi, S.; Xu, Z.; Ma, W.; Wang, Z.; Liu, S.; Gao, C. Highly Crystalline Graphene Fibers with Superior Strength and Conductivities by Plasticization Spinning. *Adv. Funct. Mater.* **2020**, 2006584.
(40) Noh, S. H.; Eom, W.; Lee, W. J.; Park, H.; Ambade, S. B.; Kim, S. O.; Han, T. H. Joule heating-induced sp2-restoration in graphene fibers. *Carbon* **2019**, *142*, 230−237.
(41) Chen, L.; He, Y.; Chai, S.; Qiang, H.; Chen, F.; Fu, Q. Toward High Performance Graphene Fibers. *Nanoscale* **2013**, *5*, 5809−5815.
(42) Kim, Y. S.; Kang, J. H.; Kim, T.; Jung, Y.; Lee, K.; Oh, J. Y.; Park, J.; Park, C. R. Easy Preparation of Readily Self-Assembled High-Performance Graphene Oxide Fibers. *Chem. Mater.* **2014**, *26*, 5549−5555.
(43) Jalili, R.; Aboutalebi, S. H.; Esrafilzadeh, D.; Shepherd, R. L.; Chen, J.; Aminorroaya-Yamini, S.; Konstantinov, K.; Minett, A. I.; Razal, J. M.; Wallace, G. G. Scalable one-step wet-spinning of graphene fibers and yarns from liquid crystalline dispersions of graphene oxide: towards multifunctional textiles. *Adv. Funct. Mater.* **2013**, *23*, 5345−5354.
(44) Ma, T.; Gao, H. L.; Cong, H. P.; Yao, H. B.; Wu, L.; Yu, Z. Y.; Chen, S. M.; Yu, S. H. A Bioinspired Interface Design for Improving the Strength and Electrical Conductivity of Graphene-Based Fibers. *Adv. Mater.* **2018**, *30*, 1706435.
(45) Kim, I. H.; Yun, T.; Kim, J. E.; Yu, H.; Sasikala, S. P.; Lee, K. E.; Koo, S. H.; Hwang, H.; Jung, H. J.; Park, J. Y.; Jeong, H. S.; Kim, S. O. Mussel-Inspired Defect Engineering of Graphene Liquid Crystalline Fibers for Synergistic Enhancement of Mechanical Strength and Electrical Conductivity. *Adv. Mater.* **2018**, *30*, 1803267.
(46) Li, M.; Zhang, X.; Wang, X.; Ru, Y.; Qiao, J. Ultrastrong Graphene-Based Fibers with Increased Elongation. *Nano Lett.* **2016**, *16*, 6511−6515.
(47) Zheng, X.; Zhou, X.; Zou, L.; Hong, S.; Yao, L.; Qiu, Y. Evaluating the Interfacial Properties of Wrinkled Graphene Fiber through Single-Fiber Fragmentation Tests. *J. Mater. Sci.* **2020**, *55*, 1023−1034.
(48) Edie, D. D.; Fain, C. C.; Robinson, K. E.; Harper, A. M.; Rogers, D. K. Ribbon-shape carbon fibers for thermal management. *Carbon* **1993**, *31*, 941−949.
(49) Li, M.; Yang, K.; Zhu, W.; Shen, J.; Rollinson, J.; Hella, M.; Lian, J. Copper-Coated Reduced Graphene Oxide Fiber Mesh-Polymer Composite Films for Electromagnetic Interference Shielding. *ACS Appl. Nano Mater.* **2020**, *3*, 5565−5574.
(50) Wan, Y. J.; Zhu, P. L.; Yu, S. H.; Sun, R.; Wong, C. P.; Liao, W. H. Graphene Paper for Exceptional EMI Shielding Performance Using Large-Sized Graphene Oxide Sheets and Doping Strategy. *Carbon* **2017**, *122*, 74−81.
(51) Sun, D.; Yan, X.; Lang, J.; Xue, Q. High Performance Supercapacitor Electrode Based on Graphene Paper via Flame-Induced Reduction of Graphene Oxide Paper. *J. Power Sources* **2013**, *222*, 52−58.
(52) Liu, Z.; Zhang, X.; Liu, C.; Li, D.; Zhang, M.; Yin, F.; Xin, G.; Wang, G. Ferroconcrete-Inspired Design of a Nonwoven Graphene Fiber Fabric Reinforced Electrode for Flexible Fast-Charging Sodium Ion Storage Devices. *J. Mater. Chem. A* **2020**, *8*, 2777−2788.

(53) Xin, G.; Zhu, W.; Yao, T.; Scott, S. M.; Lian, J. Microstructure Control of Macroscopic Graphene Paper by Electrospray Deposition and Its Effect on Thermal and Electrical Conductivities. *Appl. Phys. Lett.* **2017**, *110*, 091909.
(54) Li, P.; Yang, M.; Liu, Y.; Qin, H.; Liu, J.; Xu, Z.; Liu, Y.; Meng, F.; Lin, J.; Wang, F.; Gao, C. Continuous Crystalline Graphene Papers with Gigapascal Strength by Intercalation Modulated Plasticization. *Nat. Commun.* **2020**, *11*, 2645.
(55) Kandare, E.; Khatibi, A. A.; Yoo, S.; Wang, R.; Ma, J.; Olivier, P.; Gleizes, N.; Wang, C. H. Improving the through-thickness thermal and electrical conductivity of carbon fibre/epoxy laminates by exploiting synergy between graphene and silver nano-inclusions. *Composites, Part A* **2015**, *69*, 72−82.
(56) El-Dessouky, H. M.; Saleh, M. N. 3D woven composites: from weaving to manufacturing. In Khanna, R.; Cayumil, R. *Recent Developments in the Field of Carbon Fibers*; IntechOpen: London, 2018; pp 51−66.
(57) Zhang, W.; Yang, Q.; Deng, X.; Bai, G.; Xiao, W.; Sui, G.; Yang, X. Improved interfacial properties of carbon fiber composites by building stress transition layer with carbon nanotubes. *Adv. Polym. Technol.* **2018**, *37*, 2510−2519.
(58) Li, Z.; Xu, Z.; Liu, Y.; Wang, R.; Gao, C. Multifunctional Non-Woven Fabrics of Interfused Graphene Fibres. *Nat. Commun.* **2016**, *7*, 13684.
(59) Lin, F.; Zhu, Z.; Zhou, X.; Qiu, W.; Niu, C.; Hu, J.; Dahal, K.; Wang, Y.; Zhao, Z.; Ren, Z.; Litvinov, D.; Liu, Z.; Wang, Z. M.; Bao, J. Orientation Control of Graphene Flakes by Magnetic Field: Broad Device Applications of Macroscopically Aligned Graphene. *Adv. Mater.* **2017**, *29*, 1604453.
(60) Fang, B.; Chang, D.; Xu, Z.; Gao, C. A Review on Graphene Fibers: Expectations, Advances, and Prospects. *Adv. Mater.* **2020**, *32*, 1902664.
(61) Zhou, Y.; Chen, C.; Zhu, S.; Sui, C.; Wang, C.; Kuang, Y.; Ray, U.; Liu, D.; Brozena, A.; Leiste, U. H.; Quispe, N. A printed, recyclable, ultra-strong, and ultra-tough graphite structural material. *Mater. Today* **2019**, *30*, 17−25.
(62) Wu, X.; Tang, L.; Zheng, S.; Huang, Y.; Yang, J.; Liu, Z.; Yang, W.; Yang, M. Hierarchical unidirectional graphene aerogel/polyaniline composite for high performance supercapacitors. *J. Power Sources* **2018**, *397*, 189−195.
(63) Yang, M.; Zhao, N.; Cui, Y.; Gao, W.; Zhao, Q.; Gao, C.; Bai, H.; Xie, T. Biomimetic architectured graphene aerogel with exceptional strength and resilience. *ACS Nano* **2017**, *11*, 6817−6824.

https://dx.doi.org/10.1021/accountsmr.0c00053
Acc. Mater. Res. 2021, 2, 7−20